Published in final edited form as:
Curr Biol. 2010 April 27; 20(8): 697–702. doi:10.1016/j.cub.2010.02.058.

Motor Coordination Via Tug-Of-War Mechanism Drives Bidirectional Vesicle Transport

Adam G. Hendricks[1,*], **Eran Perlson**[1,*], **Jennifer L. Ross**[2,*], **Harry W. Schroeder III**[1], **Mariko Tokito**[1], and **Erika L. F. Holzbaur**[1]

[1] Department of Physiology and Pennsylvania Muscle Institute, University of Pennsylvania School of Medicine, Philadelphia, PA 19104-6085, USA

[2] Department of Physics, University of Massachusetts, Amherst, MA 01003, USA

Summary

The microtubule motors kinesin and dynein function collectively to drive vesicular transport. High resolution tracking of vesicle motility in the cell indicates that transport is often bidirectional, characterized by frequent directional changes. However, the mechanisms coordinating the collective activities of oppositely-oriented motors bound to the same cargo are not well understood. To examine motor coordination, we purified neuronal transport vesicles and analyzed their motility using automated particle tracking with nanometer resolution. The motility of purified vesicles reconstituted in vitro closely models the movement of Lysotracker-positive vesicles in primary neurons, where processive bidirectional motility is interrupted with frequent directional switches, diffusional movement and pauses. Quantitative analysis indicates that vesicles co-purify with a low number of stably-bound motors: 1–5 dynein and 1–4 kinesin motors. These observations compare well to predictions from a stochastic tug-of-war model, where transport is driven by the force-dependent kinetics of teams of opposing motors in the absence of external regulation. Together, these observations indicate that vesicles move robustly with a small complement of tightly-bound motors, and suggest an efficient regulatory scheme for bidirectional motility where small changes in the number of engaged motors manifest in large changes in the motility of cargo.

Results

High resolution tracking of vesicle movements in the cell has shown that in many instances transport along the microtubule (MT) cytoskeleton is bidirectional (reviewed in [1]. Here, we investigate the mechanisms underlying bidirectional transport to address the questions: (1) Are opposing motors simultaneously bound to cargos and engaged in active transport, or are motors of only one type/directionality active at a time? and (2) Is directionality determined through external regulation (e.g. via effectors, binding partners, or post-translational modifications) or a result of the unregulated force-dependent kinetics of cargo-bound motors?

Corresponding author: Erika L. F. Holzbaur, University of Pennsylvania, D400 Richards Building, 3700 Hamilton Walk, Philadelphia, PA 19104-6085., T: (215) 573-3257, F: (215) 573-5851, holzbaur@mail.med.upenn.edu.

[*]The first three authors contributed equally to this work.

In order to reconstitute bidirectional transport in vitro, we isolated neuronal transport vesicles from a transgenic mouse expressing low levels of the dynactin subunit dynamitin fused to GFP. In this line, GFP-dynamitin is efficiently incorporated into dynactin, without altering the motility of the purified dynein-dynactin motor complex [2]. In neurons from these mice, GFP-labeled dynactin is localized in a punctate pattern in the cell soma and axon of neurons *in situ* and in culture (Fig. 1A), consistent with the possible integration of the labeled protein into membrane-associated dynactin complexes.

We isolated membranous vesicles by differential centrifugation followed by flotation through a discontinuous sucrose density gradient [3]. Analysis of the purified vesicle fraction demonstrates the co-purification of MT motors dynein, kinesin-1, and kinesin-2 along with dynactin, including the GFP-labeled dynamitin subunit (Fig. 1B). Thus, a complement of motor proteins remains tightly-associated with the vesicles throughout the purification.

Proteins known to localize to the axonal transport compartment, such as synaptotagmin and synaptophysin, are also enriched in the isolated vesicles, as well as markers for late endosomes/lysosomes, including LAMP-1 and Rab 7. In contrast, Rab 5, a marker for early endosomes, is not preferentially enriched in this vesicle preparation (Fig. 1B). We used electron microscopy to examine negatively stained preparations of vesicles bound to MTs (Fig. 1C). Vesicles had a mean diameter of 90.0 ± 2.9 nm (± SEM, n>300), consistent with previously characterized axonal transport vesicles (50–150 nm) [4,5].

Photobleaching was used to quantify the number of bound GFP-dynamitin molecules stably associated with purified vesicles. GFP-dynamitin integrates into dynactin at a ratio of 2.2 labeled subunits out of four total dynamitin subunits per complex [2]. Quantitative stepwise photobleaching of dispersed vesicles statically bound to the cover glass results in a bimodal distribution (Fig. 1D,S1A). The majority of the vesicles (69%) were quenched in fewer than 10 steps, while 31% of the population was quenched in 10 to 20 steps. A fraction of the population was very bright (>20 bleaches); this likely correlates with vesicle aggregates seen by EM that did not bind well to MTs in motility assays, and were excluded from further analysis. Given a mean of 7.6 ± 3.0 (±SD) bleaching steps per dispersed vesicle, we estimate that on average, 3.5 ± 1.9 (±SD) dynactin molecules are bound to each vesicle.

The ratio of dynactin, kinesin-1, and kinesin-2 to dynein was measured by quantitative blotting of purified vesicle fractions, comparing multiple independent vesicle preparations to dilution series of purified recombinant standards (Fig. 1E,S1B,C). We measured a ratio of 1.3 ± 0.1 (± SEM, P=0.01, n=3 independent vesicle preps) for dynactin to dynein, similar to the recently reported 1:1 stoichiometry of dynein to dynactin in yeast [6]. We found an average ratio of 0.16 ± 0.02 (± SEM, P=0.01, n=3 preps) for kinesin-1:dynein and a ratio of 0.63 ± 0.04 (± SEM, P=0.004, n=3) for kinesin-2:dynein. Combined, quantitative western blotting and photobleaching yield an estimate of 2.8 ± 1.6 (± SD) dynein molecules, 3.5 ± 1.9 dynactin molecules, 0.45 ± 0.27 kinesin-1 molecules, and 1.7 ± 1.0 kinesin-2 molecules per vesicle. These measurements of the number of *total* cargo-bound motors are remarkably similar to previous estimates for the numbers of *engaged* motors driving vesicle transport in vivo, which range from 1 to 4 for kinesin and 1 to 5 for dynein [4,7–11]. Together, these results suggest that multiple motor types are stably bound to vesicles moving along neuronal processes, and that oppositely-directed MT motors are bound to cargo at low, but similar, numbers.

To analyze the motility of GFP-labeled vesicles along rhodamine-labeled MTs in vitro, we used TIRF microscopy with 16.3-nanometer resolution (Fig. 2A). Purified vesicles show ATP-sensitive binding to MTs (Fig. 3A,S3A). AMPPNP induced the stable binding of

>70% of the vesicles to MTs, consistent with the formation of a rigor bond via kinesin. Depletion of ATP also leads to the formation of a rigor bond between the vesicle and the MT, presumably due to trapping of dynein in the strongly-bound, no nucleotide state.

Automated tracking allows us to observe the motility of the vesicle population as a whole, as well as to categorize subsets of motility within the population. Tracking of individual vesicles moving along MTs demonstrates that vesicles frequently change direction, with 86% of purified vesicles switching direction during an observation time of 40 seconds (Fig. S3B). An individual vesicle may often exhibit intervals of stationary, diffusive, and processive movement. To characterize intervals of each type of bidirectional motility within runs, we used the absolute value of run length between reversals, $|L_{\mathrm{Rev}}|$ (see Fig. 2B). Characterization of motility based on $|L_{\mathrm{Rev}}|$ is consistent with the standard definitions based on mean-squared displacement [12], as shown in Fig. S2.

Next, we compared the movement of purified vesicles along MTs in vitro to the motility of vesicles in live cells. We labeled vesicles in primary cultures of cortical neurons with Lysotracker, which preferentially labels late endosomal/lysosomal compartments, as the purified vesicles used in this study are enriched for markers of this compartment. Again, we analyzed motility using automated tracking to obtain unbiased sampling with the same spatial and temporal resolution as our in vitro assays (Fig. 2C). We find that there is a close correlation between parameters of motility observed in reconstitution assays and endogenous vesicles moving in live cells (Fig. 2). Processive motility occurs with approximately equal probability in either direction for both Lysotracker-positive vesicles in live cells and purified vesicles in vitro (Fig. 2E). In vitro, average velocities of processive runs were similar in either direction (Fig. 2F,G); consistent with rates measured for soluble motor proteins in single molecule assays [13]. Velocities observed for processive runs of vesicles in cells were somewhat higher (Fig. 2F,G) possibly due to differences between the in vitro and intracellular environment, such as nucleotide concentration or ionic strength. However, like the purified vesicles in vitro, Lysotracker-positive vesicles move with comparable velocities in both directions along processes. Both in vitro and in cells, ~20% of the total vesicle population was stationary, while a large fraction displayed apparently diffusive movement, defined by short run lengths between reversals and a linear dependence of MSD on time (slope of 1 in the log-log plot) (Fig. 2D, S2).

To further probe the interactions of opposite-polarity motors involved in bidirectional motility, we observed the effects of inhibitory antibodies to dynein and dynactin on vesicle binding and motility. Addition of polyclonal antibodies to dynein heavy chain (pAb-DHC) or intermediate chain (pAb-DIC) reduced vesicle binding compared to controls, 25% ($P<0.05$) and 40% ($P<0.005$) respectively (Fig. 3B). Both pAb-DHC and a monoclonal anti-dynein antibody (mAb-DIC) increased the relative fraction of processive motility without affecting velocity (Fig. S3E,I). In contrast, addition of pAb-DHC resulted in a change in the directional bias of processive motility, with 68% of processive motion directed toward the MT plus-end in the presence of the antibody (Fig. S3G). Statistical analysis of data from individual tracks indicates that this is a significant change from controls ($P<0.0085$, $n=43$).

To examine the role of dynactin in vesicle motility, we used antibodies to the CAP-Gly domain of the $p150^{Glued}$ subunit of dynactin (mAb-p150), and a polyclonal antibody that binds to the extended coiled-coil domain of $p150^{Glued}$ (pAb-p150). Addition of mAb-p150 significantly decreased the binding of vesicles to MTs (~90% compared to controls, $P<0.0001$; Fig. 3C), suggesting that the CAP-Gly domain of dynactin may play a key role in mediating an initial association of the vesicle with the MT. A second inhibitory polyclonal antibody to dynactin (pAb-p150) also decreased vesicle binding to the MT ($P<0.05$). Of the vesicles that did bind in the presence of the anti-CAP-Gly Ab (mAb-p150), there was a

noticeable increase in the extent of processive motility along the MT as compared to controls (Fig. S3F). MT pelleting assays indicate that this Ab effectively inhibits the direct, nucleotide-independent binding of dynactin to MTs (Fig. S3K,L), but does not block the dynein-dynactin association (data not shown). Thus, the CAP-Gly domain of dynactin is likely to mediate some of the diffusive motion of vesicles along MTs observed in our in vitro assay. siRNA depletion and reconstitution experiments have shown that loss of this domain does not affect organelle distribution or rates of organelle motility in nonpolarized cells grown in culture [14,15]. However, the CAP-Gly domain may mediate an initial interaction of vesicles with MTs [16] and therefore enhance the efficiency of vesicle transport, a possibility consistent with the observations reported here.

Several antibodies to kinesin-1 were tested including an antibody known to inhibit kinesin-1 motility in vitro (SUK4, [17]). None of antibodies to kinesin-1 tested had an apparent effect on vesicle binding. In contrast, an antibody to kinesin-2 (K2.4) strongly inhibited the binding of vesicles to MTs (Fig. 3D). The population of isolated vesicles described here are Rab7-positive (Fig. 1B) and kinesin-2 has been identified as the primary anterograde motor for late endosomes [18–20]. These data suggest that the plus end-directed transport of these vesicles is driven primarily by kinesin-2.

Bidirectional motility along a MT has been modeled as a stochastic “tug-of-war” [21], whereby net transport is a consequence of the force-dependent dissociation kinetics of opposing motors in the absence of external regulation. By varying the number of plus- and minus-end directed motors or the kinetic parameters of the motors, the predicted patterns of transport exhibit a range of motility regimes; including bidirectional motility and unidirectional movement. We fit a mathematical model of bidirectional motility to our data using experimentally defined parameters for transport mediated by kinesin-1 and dynein [21] or kinesin-2 and dynein (Table S1), varying only the number of active plus- and minus-end directed motors. The results from this modeling predict that directionality is strongly modulated by the ratio of oppositely directed motors (Fig. 4A).

The predictions of the model were then compared to our experimental observations of processive motility (Fig. 4B, control); the model best describes the data when transport is driven by a ratio of 7 dynein to 1 kinesin-1 motor, or 3 dynein to 2 kinesin-2 motors. These predictions for the number of active motors are remarkably consistent with the experimental estimates for the ratio of total motors bound to vesicles, of 6:1 for dynein:kinesin-1 and 3:2 for dynein:kinesin-2.

We also compared the experimental observations on the effect of inhibitory antibodies to dynein to theoretical predictions in which a constant number of kinesins oppose a variable number of active dynein motors (Fig. 4B). The model results suggest that addition of the pAb-DHC Ab effectively decreases the number of active dynein motors. Simulated trajectories were calculated for vesicles in the absence (control) or presence of the inhibitory pAb-DHC Ab. There is also a notable qualitative correlation between the observed and simulated trajectories (Fig. 4C), again suggesting that the model provides a good fit to our observations.

Discussion

Single molecule studies on individual motors have provided significant insights into motor function (reviewed in [1,13]). However, in the cell multiple motor types interact collectively to drive bidirectional transport of cargos. Here, we purified endogenous vesicles along with their native complement of motors. These vesicles, in the absence of additional cytosolic

regulatory factors, move bidirectionally along MTs in vitro and closely model the motility of Lysotracker-labeled vesicles in neurons.

Several models have been proposed to describe the bidirectional motion of cargo in the cell [8]. Muller et al. [21] developed a mathematical model of a stochastic “tug-of-war” in which bidirectional transport is regulated by the force-dependent kinetics of opposite-directed motors, in the absence of external factors. Here we show that this model accurately describes the fast switching between plus- and minus-end directed transport exhibited by vesicles in vitro (Fig. 4). Further, we find that the number of active kinesin and dynein motors predicted by the model closely correlates with estimates of the total number of bound motors through photobleaching and quantitative western blotting. Thus, the model suggests that bidirectional motility directly results from the unregulated interactions of oppositely-directed motor proteins simultaneously bound to the same cargo. In striking agreement with our findings, Soppina et al. [11] used optical trapping to estimate the number of motors driving the transport of Dictyostelium endosomes; 4–8 “weak” dynein motors (~1 pN stall force) and a single “strong” kinesin motor (~5–6 pN stall force) drive each ~500–1500 nm endosome. However, in contrast to the behavior of the larger Dictyostelium endosomes, we did not observe “triphasic” reversals and fission events in our purified vesicles in vitro or Lysotracker-positive organelles in live cells, suggesting these characteristics may be specific to certain cargos.

Analysis of the motility of Lysotracker-positive organelles in live cells indicates that bidirectional motility, characterized by frequent directional switches and pauses, is a common transport mechanism for at least some types of intracellular cargo. Both in vitro and in cells, we also see that significant fractions of the total vesicle population are either paused or moving diffusionally over short distances. Tracking of vesicles in live cells also reveals that in addition to bidirectional motility, a subset of vesicles move primarily unidirectionally, in either the anterograde or retrograde directions (data not shown). This subset of fast, directed motility observed in the cell was not seen in vitro, suggesting that additional regulatory factors are required to reconstitute long, unidirectional runs.

Intracellular regulation may occur through several pathways. Enhanced recruitment of one motor type to a cargo would result in a directional bias. Alternatively, scaffolding molecules have been proposed to regulate motors on cargo. Directional switching may also be regulated at the level of motor activity, whereby the activity of the motors is stochastically modulated to affect the net direction of motion (Fig. 4D). Kinesin-1 can fold into an inhibited conformation [22]; intramolecular autoinhibition through folding has also been demonstrated for other members of the kinesin superfamily [23]. While binding to cargo was initially proposed to unfold kinesin and activate motility, recent progress indicates that activation occurs in multiple steps [24,25] and thus even kinesin motors tightly associated with cargo may alternate between active and inactive conformations.

Unlike for kinesin, no self-regulation scheme has been demonstrated for dynein-dynactin, suggesting only a single motor type may be actively regulated. In a dynein-dragging model, kinesin is regulated by auto-inhibition but dynein remains constitutively active. Because dynein is both less powerful and more flexible than kinesin motors, and can stay associated with the MT track even in the presence of obstacles [26], dynein could potentially enhance the processivity of cargos moving in either direction. Importantly, force measurements indicate that the stall forces of either kinesin-1 (~6 pN; reviewed in [1]) or kinesin-2 (~4 pN; our unpublished data) are significantly stronger than the opposing force of a mammalian dynein motor (~1.1 pN; [27]). Thus at a ratio of 1 kinesin-1 to 7 dynein motors or 2 kinesin-2 to 3 dynein motors, forces in either direction are balanced, and would be predicted

to result in a tug-of-war with approximately equal fractions of plus- and minus-ended motility such as we observed.

In the cell, regulation of bidirectional transport likely occurs at many levels (Fig. 4D). At long timescales, motor recruitment and/or inhibition modulates the number of active motors, biasing the "tug of war" between directed retrograde and anterograde transport, and bidirectional movement. At the short timescales within each motility regime, transport is driven by the subset of active motors via a stochastic "tug-of-war" mechanism. Accordingly, our observations that vesicles move robustly with a small complement of motors suggests an efficient regulatory scheme where small changes in the number of engaged motors manifest in large changes in the motility of the cargo.

Experimental Procedures

Detailed information on methods is provided in the SI. Briefly, we purified vesicles from transgenic mice expressing GFP-dynamitin [2]. Quantitative western blotting of multiple vesicle preparations was compared to purified recombinant DIC, dynamitin, KHC, or kinesin-2. Quantitative photobleaching was performed on dispersed fluorescent spots [2] corresponding to individual vesicles. Motility assays were performed with isolated vesicles and MTs polymerized from purified tubulin using TIRF microscopy [3]. Mathematical modeling was performed using experimentally-derived parameters for kinesin-1 and dynein [21] and estimated parameters for kinesin-2 (Table S1). The number of plus- and minus-end directed motors was varied in the model, and the predicted motility and trajectories [28] were compared to observations from in vitro vesicle transport assays.

Highlights

- Axonal transport vesicles purify with a low number of stably-bound motors.
- Vesicles move bidirectionally in vitro and in live cells.
- Directional switching during processive motility is frequent and stochastic.
- Model: tug-of-war between opposing motors in the absence of external regulation.

Supplementary Material

Refer to Web version on PubMed Central for supplementary material.

Acknowledgments

The authors acknowledge the scientific generosity of Drs. Y. Goldman, W. Hancock, V. Rodionov, V. Gelfand, and F. Ruhnow, and funding from: NIH GM48661 to ELFH, NIH 1F32GM075754 to JLR, NIH GM-071339 to HWS, and NSF NSEC DMR04-25780 and NIH GM087253 to support the microscope facility.

References

1. Holzbaur EL, Goldman YE. Coordination of molecular motors: from in vitro assays to intracellular dynamics. Curr Opin Cell Biol. 22:4–13. [PubMed: 20102789]
2. Ross JL, Wallace K, Shuman H, Goldman YE, Holzbaur EL. Processive bidirectional motion of dynein-dynactin complexes in vitro. Nat Cell Biol. 2006; 8:562–570. [PubMed: 16715075]
3. Caviston JP, Ross JL, Antony SM, Tokito M, Holzbaur EL. Huntingtin facilitates dynein/dynactin-mediated vesicle transport. Proc Natl Acad Sci U S A. 2007; 104:10045–10050. [PubMed: 17548833]

4. Miller RH, Lasek RJ. Cross-bridges mediate anterograde and retrograde vesicle transport along microtubules in squid axoplasm. J Cell Biol. 1985; 101:2181–2193. [PubMed: 2415536]
5. Cui B, Wu C, Chen L, Ramirez A, Bearer EL, Li WP, Mobley WC, Chu S. One at a time, live tracking of NGF axonal transport using quantum dots. Proc Natl Acad Sci U S A. 2007; 104:13666–13671. [PubMed: 17698956]
6. Kardon JR, Reck-Peterson SL, Vale RD. Regulation of the processivity and intracellular localization of Saccharomyces cerevisiae dynein by dynactin. Proc Natl Acad Sci U S A. 2009; 106:5669–5674. [PubMed: 19293377]
7. Ashkin A, Schutze K, Dziedzic JM, Euteneuer U, Schliwa M. Force generation of organelle transport measured in vivo by an infrared laser trap. Nature. 1990; 348:346–348. [PubMed: 2250707]
8. Gross SP. Hither and yon: a review of bi-directional microtubule-based transport. Phys Biol. 2004; 1:R1–11. [PubMed: 16204815]
9. Shubeita GT, Tran SL, Xu J, Vershinin M, Cermelli S, Cotton SL, Welte MA, Gross SP. Consequences of motor copy number on the intracellular transport of kinesin-1-driven lipid droplets. Cell. 2008; 135:1098–1107. [PubMed: 19070579]
10. Sims PA, Xie XS. Probing dynein and kinesin stepping with mechanical manipulation in a living cell. Chemphyschem. 2009; 10:1511–1516. [PubMed: 19504528]
11. Soppina V, Rai AK, Ramaiya AJ, Barak P, Mallik R. Tug-of-war between dissimilar teams of microtubule motors regulates transport and fission of endosomes. Proc Natl Acad Sci U S A. 2009; 106:19381–19386. [PubMed: 19864630]
12. Nelson SR, Ali MY, Trybus KM, Warshaw DM. Random walk of processive, quantum dot-labeled myosin Va molecules within the actin cortex of COS-7 cells. Biophys J. 2009; 97:509–518. [PubMed: 19619465]
13. Ross JL, Ali MY, Warshaw DM. Cargo transport: molecular motors navigate a complex cytoskeleton. Curr Opin Cell Biol. 2008; 20:41–47. [PubMed: 18226515]
14. Kim H, Ling SC, Rogers GC, Kural C, Selvin PR, Rogers SL, Gelfand VI. Microtubule binding by dynactin is required for microtubule organization but not cargo transport. J Cell Biol. 2007; 176:641–651. [PubMed: 17325206]
15. Dixit R, Levy JR, Tokito M, Ligon LA, Holzbaur EL. Regulation of dynactin through the differential expression of p150Glued isoforms. J Biol Chem. 2008; 283:33611–33619. [PubMed: 18812314]
16. Vaughan PS, Miura P, Henderson M, Byrne B, Vaughan KT. A role for regulated binding of p150(Glued) to microtubule plus ends in organelle transport. J Cell Biol. 2002; 158:305–319. [PubMed: 12119357]
17. Ingold AL, Cohn SA, Scholey JM. Inhibition of kinesin-driven microtubule motility by monoclonal antibodies to kinesin heavy chains. J Cell Biol. 1988; 107:2657–2667. [PubMed: 2974459]
18. Loubery S, Wilhelm C, Hurbain I, Neveu S, Louvard D, Coudrier E. Different microtubule motors move early and late endocytic compartments. Traffic. 2008; 9:492–509. [PubMed: 18194411]
19. Brown CL, Maier KC, Stauber T, Ginkel LM, Wordeman L, Vernos I, Schroer TA. Kinesin-2 is a motor for late endosomes and lysosomes. Traffic. 2005; 6:1114–1124. [PubMed: 16262723]
20. Bananis E, Nath S, Gordon K, Satir P, Stockert RJ, Murray JW, Wolkoff AW. Microtubule-dependent movement of late endocytic vesicles in vitro: requirements for Dynein and Kinesin. Mol Biol Cell. 2004; 15:3688–3697. [PubMed: 15181154]
21. Muller MJ, Klumpp S, Lipowsky R. Tug-of-war as a cooperative mechanism for bidirectional cargo transport by molecular motors. Proc Natl Acad Sci U S A. 2008; 105:4609–4614. [PubMed: 18347340]
22. Stock MF, Guerrero J, Cobb B, Eggers CT, Huang TG, Li X, Hackney DD. Formation of the compact confomer of kinesin requires a COOH-terminal heavy chain domain and inhibits microtubule-stimulated ATPase activity. J Biol Chem. 1999; 274:14617–14623. [PubMed: 10329654]

23. Imanishi M, Endres NF, Gennerich A, Vale RD. Autoinhibition regulates the motility of the C. elegans intraflagellar transport motor OSM-3. J Cell Biol. 2006; 174:931–937. [PubMed: 17000874]

24. Blasius TL, Cai D, Jih GT, Toret CP, Verhey KJ. Two binding partners cooperate to activate the molecular motor Kinesin-1. J Cell Biol. 2007; 176:11–17. [PubMed: 17200414]

25. Hackney DD, Baek N, Snyder AC. Half-site inhibition of dimeric kinesin head domains by monomeric tail domains. Biochemistry. 2009; 48:3448–3456. [PubMed: 19320433]

26. Dixit R, Ross JL, Goldman YE, Holzbaur EL. Differential regulation of dynein and kinesin motor proteins by tau. Science. 2008; 319:1086–1089. [PubMed: 18202255]

27. Mallik R, Carter BC, Lex SA, King SJ, Gross SP. Cytoplasmic dynein functions as a gear in response to load. Nature. 2004; 427:649–652. [PubMed: 14961123]

28. Gillespie DT. A general method for numerically simulating the stochastic time evolution of coupled chemical reactions. Journal of Computational Physics. 1976; 22:403–434.

29. Muthukrishnan G, Zhang Y, Shastry S, Hancock WO. The processivity of kinesin-2 motors suggests diminished front-head gating. Curr Biol. 2009; 19:442–447. [PubMed: 19278641]

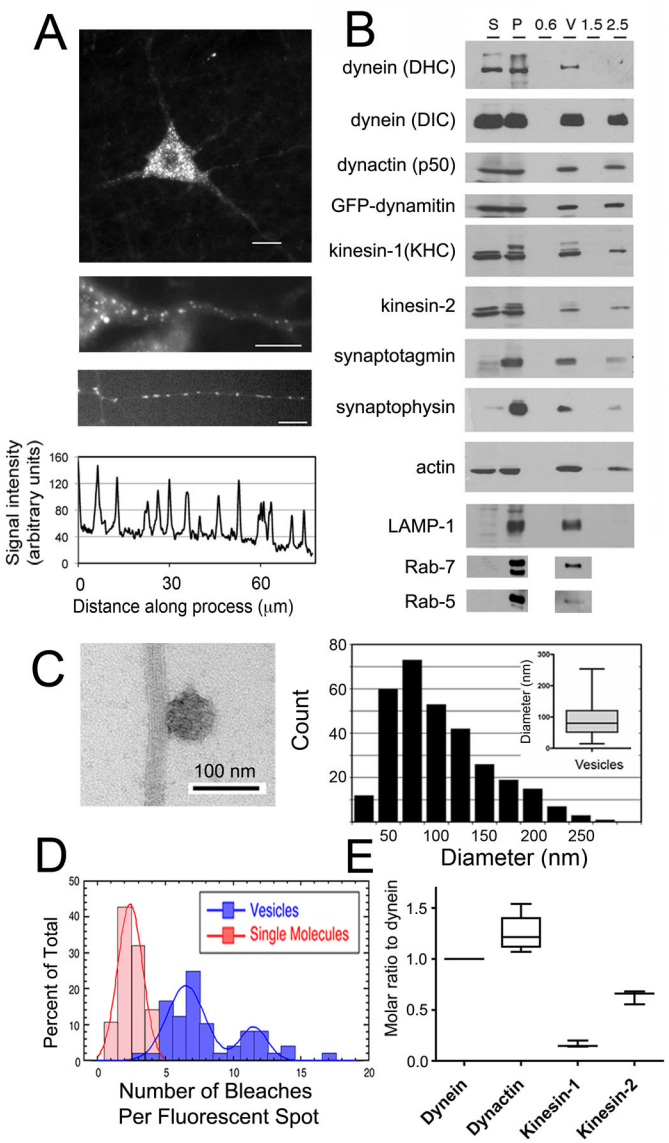

Fig. 1. MT motor proteins dynein and kinesin co-purify with axonal transport vesicles and drive active motility in vitro

(A) *Top*, GFP-dynamitin is distributed in a punctate pattern throughout the cell soma and processes of motor neurons in vivo. *Middle*, GFP-dynamitin is localized to vesicles distributed along the axon of a motor neuron in vivo. *Bottom*, GFP-dynamitin is distributed to vesicles along the processes of DRG neurons cultured from $Tg^{GFP\text{-}dynamitin}$ mice. A corresponding line scan of relative fluorescent intensity along the neurite emphasizes the punctate nature of the localization. (B) MT motor proteins cytoplasmic dynein (DHC and DIC), kinesin-1 (KHC), and kinesin-2, and dynactin (p50), axonal transport markers synaptotagmin and synaptophysin, and late endosome markers LAMP-1 and Rab-7 co-purify with isolated vesicles. GFP-labeled dynamitin is efficiently incorporated into the vesicle-associated dynactin complex. Fractions from the vesicle purification include initial cytosolic (S) and membrane (P) fractions from mouse brain homogenate and the 0.6 M (0.6), the 0.6/1.5 M (V), and 1.5 M and 2.5 M (1.5 and 2.5) steps from a discontinuous sucrose gradient. (C) Vesicles isolated from the 0.6/1.5 M interface were incubated with MTs and analyzed by negative stain EM (left panel). Vesicles had a mean diameter of 90.0 ± 2. 9 nm

(SE, n=311). (D) Stepwise quantitative photobleaching of dispersed vesicles produced a bimodal distribution. For comparison, photobleaching data for soluble purified dynein/dynactin [2] is shown (red bars). (E) Quantitative western blotting was performed to measure vesicle-bound cytoplasmic dynein, dynactin, kinesin-1 and kinesin-2.

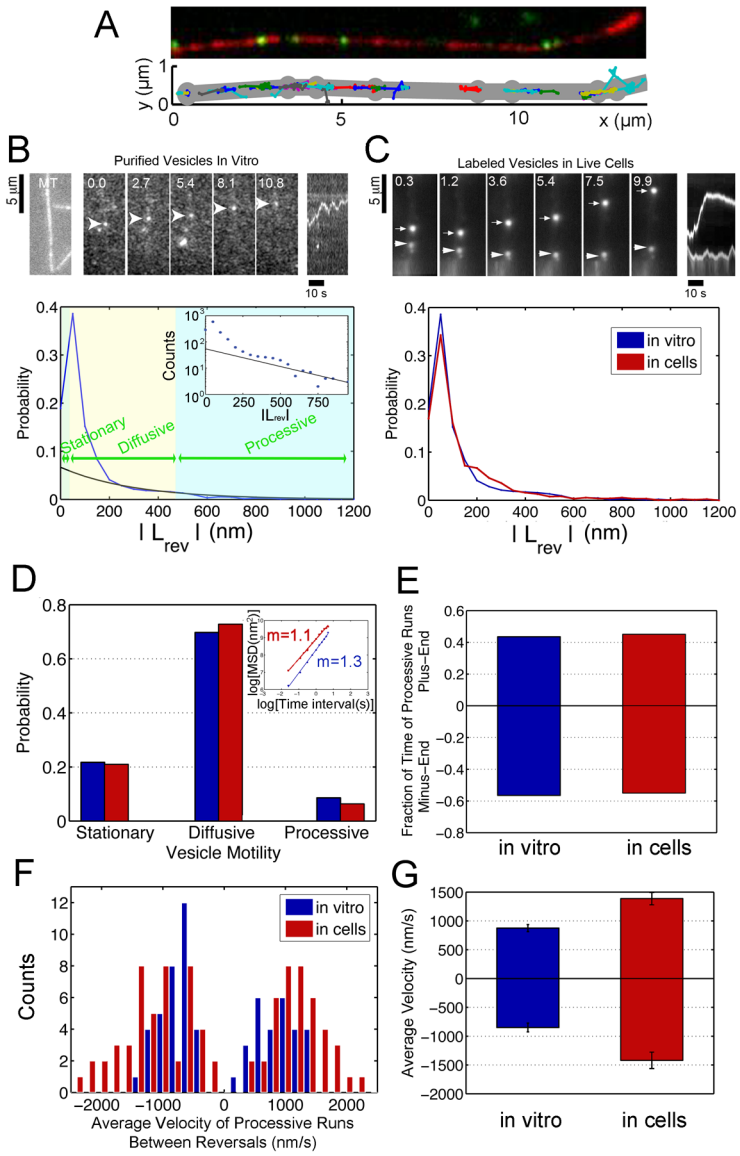

Fig. 2. Bidirectional transport of purified vesicles along MTs in vitro closely models the motility of Lysotracker-positive vesicles in live cells

(A) Automated tracking analysis of in vitro motility. *Top*: Fluorescent vesicles (in green) moving on a polarity-marked MT (in red, plus end is bright). *Bottom*: Custom Matlab programs were used to automatically track the vesicles. The MT coordinates (in gray) were tracked manually in ImageJ. (B) The top left panels show a rhodamine-labeled MT and a time series of the movement of a GFP-labeled vesicle along the MT. A kymograph of distance moved over time is shown in the top right panel. The bottom panel shows the distribution of absolute values of run lengths between reversals, $|L_{Rev}|$, from automated tracking of the vesicle population as a whole (blue curve). Intervals of motility were categorized as stationary when $|L_{Rev}| < 33$ nm (twice the standard deviation of the tracked position of an immobile vesicle attached to the coverslip). The distribution of $|L_{Rev}|$ shows a peak <100 nm corresponding primarily to vesicle diffusion. To differentiate between diffusive and processive motility, the long tail of the distribution was fit to an exponential (black curve, characteristic decay length = 300 nm, R-value = 0.8), which provides a good fit for runs >500 nm (see inset). (C) A time series and kymograph of LysoTracker-labeled

vesicles in live cells shows bidirectional motility (top). The distribution of $|L_{Rev}|$ for Lysotracker-positive vesicles and purified vesicles in vitro indicates similar motility (bottom). (D) Bidirectional motility in vitro and in the cell show a similar distribution. The corresponding MSD s for all tracked vesicles (inset) are consistent. (E) ~40% of processive motility is plus-end directed while ~60% is towards the minus end for purified vesicles and Lysotracker-labeled vesicles. (F) Distribution of observed velocities for processive motility of vesicles in vitro (100 μM ATP) and in live cells. (G) The average velocity of processive runs in the plus- and minus-end directions is higher for Lysotracker-labeled vesicles in live cells than for purified vesicles in vitro.

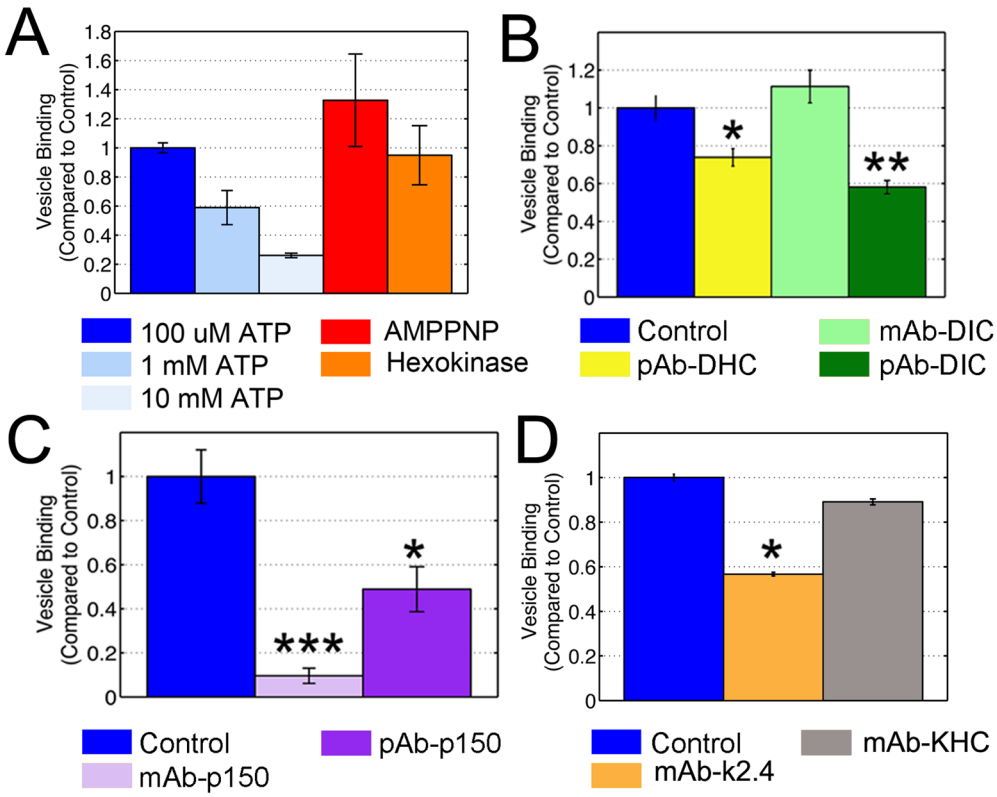

Fig. 3. Binding of vesicles to MTs is motor-driven and dependent on inhibitory antibodies to dynein, dynactin and kinesin

(A) The binding of vesicles to MTs is ATP-dependent. Addition of AMP-PNP increases binding, likely due to rigor binding of kinesin. Similarly, depletion of ATP through hexokinase increases binding, likely due to the rigor binding of dynein. (B) Antibodies (Abs) to dynein partially inhibit vesicle binding to MTs (yellow, *: P<0.05 and dark green bars, **: P<0.005). (C) Vesicle binding was inhibited by addition of either mAb-p150 (light purple, ***: P>0.0001) or pAb-p150 (dark purple, *: P>0.05). (D) Vesicle binding was inhibited by an antibody to kinesin-2 (orange, *:P>0.05). However, an antibody known to inhibit motility of kinesin-1 in vitro (SUK4, gray) did not have a significant effect on binding. The control for (B), (C), and (D) is binding in the presence of an anti-Myc antibody.

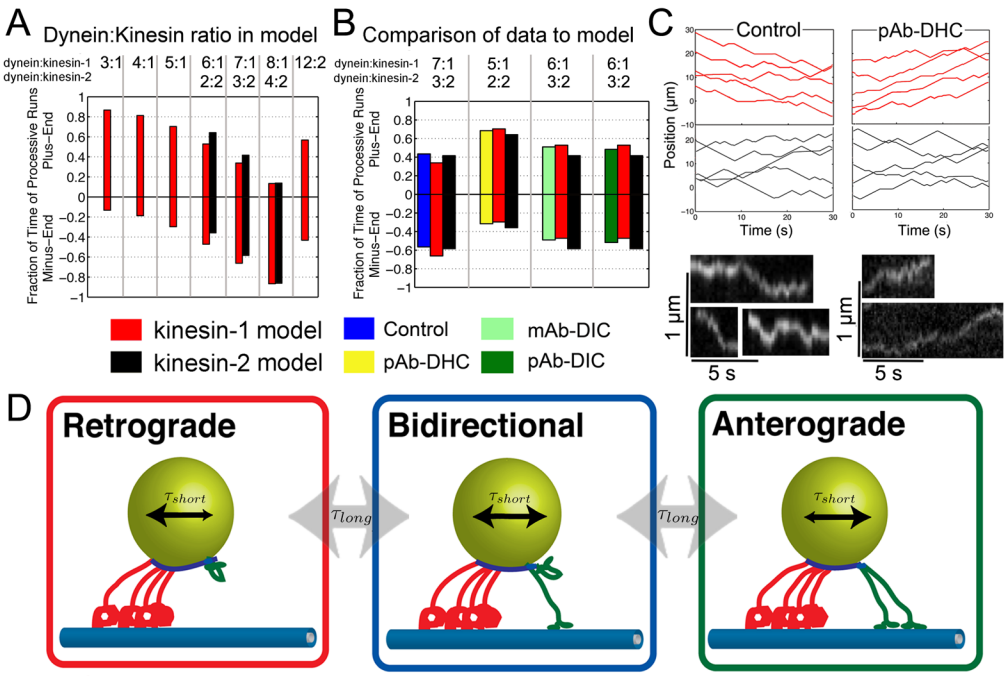

Fig. 4. A tug-of-war model predicts the observed parameters of bidirectional transport in vitro

A tug-of-war model [21] was used to analyze the observed motility of neuronal transport vesicles moving bidirectionally along MTs in vitro. Model parameters were based on previous experimental observations [21,29]. The two free parameters in the model are the number of actively engaged plus- and minus-end directed motors. (A) The relative fraction of time vesicles are moving toward either the plus or minus ends of the MT depends strongly on the ratio of the number of engaged plus- and minus-end directed motors. Predictions are shown over a range of dynein:kinesin-1 and dynein:kinesin-2 ratios. (B) Experimental data from vesicle motility along MTs is best described by a mole ratio of 7:1 dynein to kinesin-1 motors or 3:2 dynein to kinesin-2 motors. Data from vesicles treated with an Ab to DHC and DIC suggest a fraction of the dynein is inhibited under these conditions. (C) The Gillespie method [28] was used to generate simulated trajectories for control vesicles as well as vesicles incubated with pAb-DHC for motility driven by dynein and kinesin-1 (red), and dynein and kinesin-2 (black). Simulated trajectories are compared to kymographs of vesicle motility (excerpted from Fig. S4). (D) Regulation of bidirectional transport likely occurs at several levels. Recruitment, activation, or inhibition of motor proteins regulates the number of active motors associated with vesicular cargo. Regulation on a longer time scale (τ_{long}) likely involves motor effectors. At shorter time scales (τ_{short}), net directionality of movement results from a stochastic “tug-of-war” among opposing motor proteins bound to the same cargo and actively engaged with the MT.